

Stability Constants: A New Twist in Transition Metal Bispidine Chemistry

Karin Born,[†] Peter Comba,^{*,†} Rosana Ferrari,[†] Geoffrey A. Lawrance,[‡] and Hubert Wadepohl[†]

Universität Heidelberg, Anorganisch-Chemisches Institut, Im Neuenheimer Feld 270, D-69120 Heidelberg, Germany, and School of Environment and Life Sciences, University of Newcastle, Callaghan, NSW 2308, Australia

Received August 9, 2006

Transition metal complexes with 2,4-substituted tetradentate, 2,3,4- and 2,4,7-substituted pentadentate, and 2,3,4,7-substituted hexadentate bispidine ligands (bispidine = 3,7-diazabicyclo[3.3.1]nonane) with two tertiary amine and two, three, or four pyridine donors are relatively stable ($10 < \log K_{\text{CuL}} < 18$). Interestingly, the two isomeric pentadentate ligands have very different stabilities with a variety of metal ions and, depending on the metal ion, one of the isomers leads to more stable complexes than the hexadentate and the other to less stable complexes than the tetradentate ligand. Another interesting observation is that the complex stabilities of all bispidine ligands reported here do not follow the Irving-Williams series since the stability constants of the cobalt(II) complexes are up to 4 log units larger than those of the corresponding nickel(II) complexes. All these observations are analyzed on the basis of subtle distortions of the coordination geometries, and these have been related previously to Jahn–Teller-derived distortions for the copper(II) complexes. However, similar but less pronounced structural properties are observed with other metal centers, as shown, e.g., with the experimental structures of the two zinc(II) complexes with the isomeric pentadentate ligands reported here. The structural properties and the related stabilities are also discussed on the basis of force field calculations.

Introduction

There is a rich coordination chemistry of bispidine ligands (bispidine backbone: 3,7-diazabicyclo[3.3.1]nonane), and these are available in a large variety by two consecutive Mannich reactions (see Scheme 1 for the synthesis, the ligands discussed here, the atom numbering, and the generalized bispidine complex structure).¹ Structures^{2–4} and bonding,^{5,6} the electron-transfer properties,⁷ catalytic aziridination,⁸

and oxygen activation^{9–14} of bispidine transition metal complexes have been studied in detail.¹ The unique and interesting properties of bispidine coordination compounds are the result of the rigidity of the diazaadamantane-derived bispidine backbone and the typical bispidine complex structure it enforces (see Scheme 1), showing an asymmetric cis-octahedral geometry with a usually short and strong bond to the substrate X_E and a longer and weaker bond to the substrate X_A (see Scheme 1), both of which can be blocked by additional donors appended to N3 or N7. This is an important design principle for specific catalysts,¹ and it is of interest that these elongations of one axis (generally but

* To whom correspondence should be addressed. E-mail: peter.comba@aci.uni-heidelberg.de.

[†] Universität Heidelberg.

[‡] University of Newcastle.

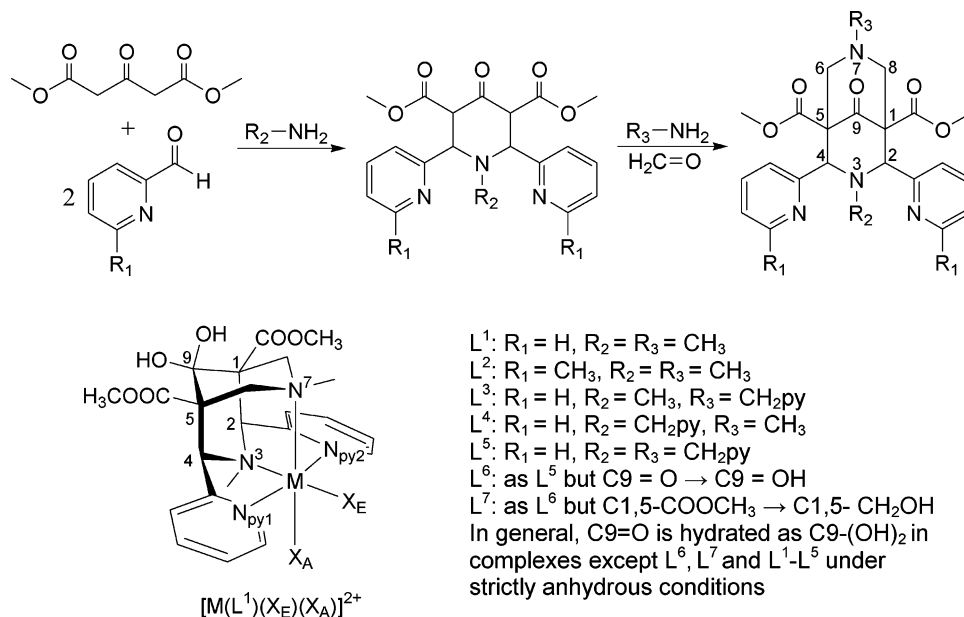
- (1) Comba, P.; Kerscher, M.; Schiek, W. *Prog. Inorg. Chem.*, in press.
- (2) Comba, P.; Kerscher, M.; Merz, M.; Müller, V.; Pritzkow, H.; Remenyi, R.; Schiek, W.; Xiong, Y. *Chem.—Eur. J.* **2002**, *8*, 5750.
- (3) Comba, P.; Kerscher, M. *Cryst. Eng.* **2004**, *6*, 197.
- (4) Comba, P.; Martin, B.; Prikhod'ko, A.; Pritzkow, H.; Rohwer, H. *C. R. Chim.* **2005**, *6*, 1506.
- (5) Comba, P.; Lienke, A. *Inorg. Chem.* **2001**, *40*, 5206.
- (6) Atanasov, M.; Comba, P.; Martin, B.; Müller, V.; Rajaraman, G.; Rohwer, H.; Wunderlich, S. *J. Comput. Chem.* **2006**, *27*, 1263.
- (7) Comba, P.; Kerscher, M.; Roodt, A. *Eur. J. Inorg. Chem.* **2004**, *23*, 4640.
- (8) Comba, P.; Merz, M.; Pritzkow, H. *Eur. J. Inorg. Chem.* **2003**, 1711.

- (9) Börzel, H.; Comba, P.; Katsichtis, C.; Kiefer, W.; Lienke, A.; Nagel, V.; Pritzkow, H. *Chem.—Eur. J.* **1999**, *5*, 1716.
- (10) Börzel, H.; Comba, P.; Pritzkow, H. *J. Chem. Soc., Chem. Commun.* **2001**, 97.
- (11) Born, K.; Comba, P.; Daubinet, A.; Fuchs, A.; Wadepohl, H. *J. Biol. Inorg. Chem.*, in press.
- (12) Bukowski, M. R.; Comba, P.; Lienke, A.; Limberg, C.; Lopez de Laorden, C.; Mas-Balleste, R.; Merz, M.; Que, L., Jr. *Angew. Chem.* **2006**, *118*, 3524; *Angew. Chem., Int. Ed.* **2006**, *45*, 3446.
- (13) Bautz, J.; Bukowski, M.; Kerscher, M.; Stubna, A.; Comba, P.; Lienke, A.; Münck, E.; Que, L., Jr. *Angew. Chem.* **2006**, *118*, 5810; *Angew. Chem., Int. Ed.* **2006**, *45*, 5681.
- (14) Bautz, J.; Comba, P.; Que, L., Jr. *Inorg. Chem.* **2006**, *45*, 7077.

Table 1. Protonation Constants, Reduction Potentials, and UV–vis dd Bands of Bispidine–Transition Metal Complexes^a

	L ¹	L ²	L ³	L ⁴	L ⁵	L ⁶	L ⁷
pK _{a1}	1.78(12)		1.86(10)	2.50(4)			1.75(12)
pK _{a2}	2.36(13)	2.98(9)	3.95(10)	5.21(4)	4.72(13)	5.52(13)	5.65(9)
pK _{a3}	9.10(9.8)	9.13(7)	7.44(8)	8.89(3)	6.68(8)	7.58(11)	8.93(5)
E°(Cu ^{II/I}) (mV) ^b	-417	-98	-603	-489	-573		
E°(Cu ^{II/I}) (mV) ^c	-425	-45	-523	-413	-502	-433	
E°(Co ^{III/II})	653		519	300	224		
dd Cu ^{II} (nm)	653(90)	621(63)	617(108)	694(47)	620(125)	573	614
dd Co ^{II} (nm)	475	585	483	453	492	395	395
	583	617	542	572	551	463	488
dd Ni ^{II} (nm)	460	630		441	467	444	
	521	641		546	525	536	525

^a Aqueous solution data except for redox potentials, which are in MeCN and H₂O. ^b In MeCN, vs Ag/AgNO₃; μ = 0.1. ^c In H₂O, vs Ag/AgCl; μ = 0.1.

Scheme 1

not exclusively N7–M–X_A) are not restricted to typical Jahn–Teller active metal centers such as copper(II); therefore, in the copper(II) complexes these might not be exclusively due to pseudo-Jahn–Teller distortions.¹⁵ The analysis of this important observation in combination with experimentally determined redox potentials and complex stabilities is the basis of the present publication. In addition to these structural properties, bispidine complexes are known to have elastic coordination geometries, i.e., flat potential energy surfaces with various shallow minima.¹ A result of this bispidine-enforced property is that various isomers with similar energies and quite different geometries usually are accessible.^{1–4,15} This provides the basis for the possibility of tuning the properties of bispidine complexes.

Here we report the solution properties, i.e., complex stabilities, redox potentials, and some ligand field spectra of a series of first row transition metal complexes of various tetra-, penta-, and hexadentate bispidine ligands. These data sets are used, together with published experimental and computed structural data, to analyze possible reasons and modes of distortion.

Table 2. Complex Stabilities (log K_{ML}) of the Metal Ion Bispidine Complexes in Aqueous Solution with μ = 0.1 M (KCl)

	log K (ML)					
	L ¹	L ²	L ³	L ⁴	L ⁵	L ⁷
Cu(I) ^a	5.61(32)	5.48(32)	5.69(22)	6.29(43)	4.97(52)	
Cu(I) ^b	9.5	8.9	9.6	8.8	7.9	
Cu(II)	16.56(5)	9.60(7)	18.31(12)	15.66(3)	16.28(10)	17.70(7)
Cu(II) ^c	12.5	7.1	15.3	14.5	16.2	
Co(II)	5.46(5)		6.23(5)	13.69(5)	7.30(6)	10.60(4)
Ni(II)		7.50(9)	6.10(8)	9.54(6)	5.02(7)	7.20(10)
Zn(II)	11.37(1)		8.28(5)	13.57(4)	9.18(5)	12.52(5)
Li(I) ^d	2.70(9)	3.90(10)		3.65(9)	3.70(8)	~3

^a By NMR titration, in MeCN. ^b Calculated in H₂O (ln(K_{Cu^I}/K_{Cu^{II}}) = E°nF/RT). ^c Calculated in CH₃CN. ^d By UV–vis titration.}}

Results and Discussion

Ligand field spectroscopic data, redox potentials, and complex stabilities of Li^I, Co^{II/III}, Ni^{II}, Cu^{I/II}, and Zn^{II} complexes of the two tetradentate (L¹, L²), two isomeric pentadentate (L³, L⁴), and a hexadentate bispidine ligand (L⁵) are listed in Tables 1 and 2. The stability constants for Co^{II}, Ni^{II}, Cu^{II}, Zn^{II}, and Li^I complexes were determined by potentiometric or combined spectrophotometric/potentiometric titrations; those for Cu^I were obtained from ¹H-NMR titrations. A typical set of ¹H-NMR spectra is given in Figure 1. All other ¹H-NMR spectroscopic data and titration curves,

(15) Comba, P.; Hauser, A.; Kerscher, M.; Pritzkow, H. *Angew. Chem., Int. Ed.* **2003**, *42*, 4536.

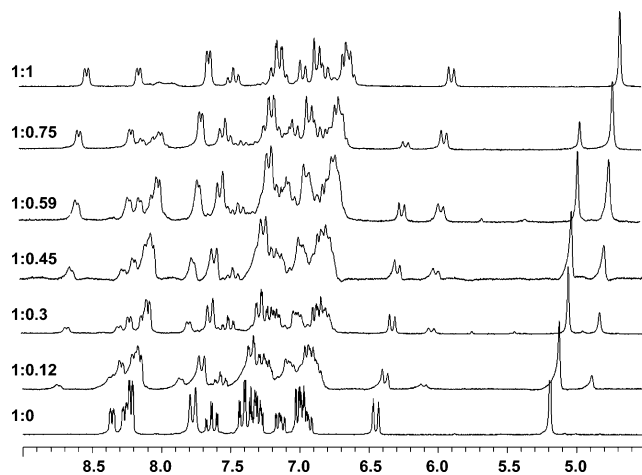


Figure 1. $^1\text{H-NMR}$ spectra of L^5 with different ratios of L^5 to Cu^{I} , from pure L^5 (bottom) to equimolar Cu^{I} and ligand concentration (top). Solvent: MeCN-d_6 .

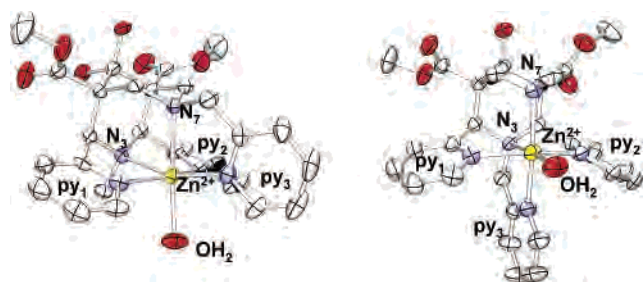


Figure 2. ORTEP plots of the X-ray crystal structures of the molecular cations of $[\text{Zn}(\text{L}^3)(\text{OH}_2)](\text{ClO}_4)_2$ (left) and $[\text{Zn}(\text{L}^4)(\text{OH}_2)](\text{ClO}_4)_2$ (right). For the atom numbering scheme see Scheme 1.

as well as the fitted equilibrium constants for species other than ML , which are listed in Table 2, are given as Supporting Information. The electronic spectra of the Co^{II} , Ni^{II} , and Cu^{II} bispidine complexes indicate that all donors are coordinated in solutions of the complexes with the penta- and hexadentate bispidine species (see Table 1). Published $^1\text{H-NMR}$ and structural data of the Cu^{I} complexes^{16,17} in combination with DFT calculations¹⁷ indicate that this is not the case with Cu^{I} .

A general observation with copper complexes is that the stability of the copper(I) compounds is roughly independent of the ligand and, therefore, there is a linear correlation of the Cu^{II} stabilities with the corresponding redox potentials with a slope of -0.059 .¹⁸ The invariance of the Cu^{I} stability constants ($\log K_{\text{Cu}^{\text{I}}} = 14.5 \pm 1.5$)¹⁸ is not well understood, and there seems to be some dependence at least from the ligand type and/or from the solvent (tetrathiamacrocycles, 80% MeOH, $\log K_{\text{Cu}^{\text{I}}} = 11.0 \pm 1.5$;¹⁹ tetrathiamacrocycles, CH_3CN , $\log K_{\text{Cu}^{\text{I}}} = 5.5 \pm 1$;²⁰ tripodal systems, H_2O , \log

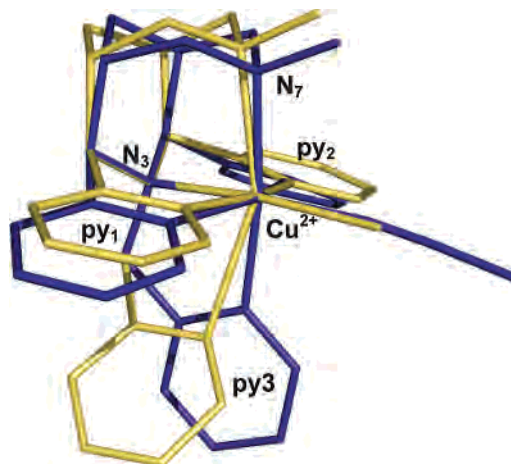


Figure 3. Overlay plot of the molecular cations $[\text{Cu}(\text{L}^4)(\text{MeCN})]^{2+}$ and $[\text{Cu}(\text{L}^4)(\text{Cl})]^+$.

$K_{\text{Cu}^{\text{I}}} = 14.5 \pm 1.5$).¹⁸ That is, linear correlations of $\log K_{\text{Cu}^{\text{II}}}$ vs E° only hold for a constant solvent and type of ligand. The solvent dependence of the Cu^{I} stability constants presented here is in good agreement with this observation and with the published data discussed above (CH_3CN , $\log K_{\text{Cu}^{\text{I}}} = 5.5 \pm 1$; H_2O , $\log K_{\text{Cu}^{\text{I}}} = 8.5 \pm 1$ (see below); the stability constants of Cu^{II} in CH_3CN and of Cu^{I} in H_2O , also shown in Table 2, were calculated based on the Nernst equation, see footnote in Table 2).

The comparably low complex stability of the methylated tetradentate ligand L^2 with copper(II), compared with that of the unmethylated ligand L^1 (7 log units difference, see Table 2), is well understood as primarily the result of partial quenching of the pseudo-Jahn–Teller distortion ($\text{Cu}^{\text{II}}\text{L}^1$: $\text{Cu}-\text{N}3 = 2.042 \text{ \AA}$, $\text{Cu}-\text{N}7 = 2.272 \text{ \AA}$, Cl^- trans to $\text{N}3$; $\text{Cu}^{\text{II}}\text{L}^2$: $\text{Cu}-\text{N}3 = 2.147 \text{ \AA}$, $\text{Cu}-\text{N}7 = 2.120 \text{ \AA}$, Cl^- trans to $\text{N}7$), and the low complex stability is paralleled by an increase of the redox potential by approximately 350 mV (see Table 1). Note that the differences in redox potentials as well as those of the Cu^{II} stability constants (due to the above-mentioned linear correlation) are solvent dependent and, to some extent, also dependent on the electrolyte (see also ref 3, see data of L^1 vs L^2 vs L^4 ; $\log K_{\text{Cu}^{\text{II}}}$, E° in $\text{H}_2\text{O}/\text{MeCN}$: L^1 , 16.6/12.5, $-425/-417$; L^2 , 9.6/7.1, $-45/-98$; L^4 , 15.7/14.5, $-413/-489$). The increase of the Cu^{II} complex stability from the tetradentate ligand L^1 to the pentadentate ligand L^3 Cu^{II} complex is of 2 log units; the stability of the Cu^{II} complex of the isomeric pentadentate ligand L^4 is about 1 log unit smaller than that of the tetradentate ligand L^1 , and that with the hexadentate ligand L^5 is similar to that of $\text{Cu}^{\text{II}}\text{L}^1$ and smaller than that of $\text{Cu}^{\text{II}}\text{L}^3$.

It is interesting to try to understand these unexpected results on the basis of the structural properties of the complexes. All copper(II) complexes of L^1 have an elongated $\text{Cu}-\text{N}7$ bond and the coligand (Cl^-) trans to $\text{N}3$ (see Table 3). Complexes with L^2 have the coligand trans to $\text{N}7$ (Cl^- or OH_2) with a slightly elongated $\text{Cu}-\text{N}3$ bond or trans to $\text{N}3$ (MeCN , see Table 3) with an elongated $\text{Cu}-\text{N}7$ bond.⁴ Copper(II) complexes of L^3 generally have an elongated $\text{Cu}-\text{N}7$ axis, except for the trinuclear $[\text{L}^3\text{Cu}-\text{NCFe}(\text{CN})_4\text{CN}-\text{CuL}^3]^+$ complex with a short $\text{Cu}-\text{NC}$ bond trans to $\text{N}7$.¹

(16) Börzel, H.; Comba, P.; Hagen, K. S.; Katsichtis, C.; Pritzkow, H. *Chem.—Eur. J.* **2000**, *6*, 914.

(17) Born, K.; Comba, P.; Kerscher, M.; Rohwer, H.; Pritzkow, H. Manuscript in preparation.

(18) Ambundo, E. A.; Deydier, M.-V.; Grall, A. J.; Agnera-Vega, N.; Dressel, L. T.; Cooper, T. H.; Heeg, N. J.; Ochrymowycz, L. A.; Rorabacher, D. B. *Inorg. Chem.* **1999**, *38*, 4233.

(19) Kakos, S. H.; Dressel, L. T.; Bushendorf, J. D.; Kotarba, C. T.; Wijetunge, P.; Kulatilleke, C. P.; McGillivray, M. P.; Chaka, G.; Heeg, M. J.; Ochrymowycz, L. A.; Rorabacher, D. B. *Inorg. Chem.* **2006**, *45*, 923.

(20) Dunn, B. C.; Ochrymowycz, L. A.; Rorabacher, D. B. *Inorg. Chem.* **1997**, *36*, 3253.

Table 3. Selected Structural Parameters of Cu^{II} and Zn^{II} Bispidine (L¹–L⁵) Complexes

	CuL ¹ (ref 9) X _E = Cl X _A = -	CuL ² (ref 16) X _E = NCCCH ₃ X _A = -	CuL ² (ref 16) X _E = - X _A = Cl	CuL ³ (ref 1) X _E = CN X _A = -	CuL ³ (ref 8) X _E = - X _A = Cl	CuL ⁴ (ref 15) X _E = NCCCH ₃ X _A = -	CuL ⁴ (ref 8) X _E = Cl X _A = -	CuL ⁵ (ref 21)	ZnL ¹ (ref 2) X _E = Cl X _A = -	ZnL ^{3 a} X _E = - X _A = H ₂ O	ZnL ^{4 a} X _E = H ₂ O X _A = -	ZnL ⁵ (ref 21)
M–N3	2.042(3)	2.004(4)	2.147(3)	2.048	2.036(2)	2.105(2)	2.070(2)	2.087(3)	2.192(2)	2.186(2)	2.176(3)	2.166(2)
M–N7	2.273(3)	2.376(4)	2.120(3)	2.107	2.368(2)	2.106(2)	2.478(2)	2.045(3)	2.103(2)	2.295(2)	2.197(3)	2.234(2)
M–py1	2.024(3)	2.075(4)	2.061(3)	2.556	2.028(2)	2.353(2)	2.011(2)	2.280(3)	2.092(2)	2.113(2)	2.189(3)	2.170(2)
M–py2	2.020(3)	2.052(4)	2.064(3)	2.371	2.029(2)	2.260(2)	1.987(2)	2.573(3)	2.124(2)	2.173(2)	2.192(3)	2.285(2)
M–X _E	2.232(1)	1.950(5)		2.056	2.029(2)	2.015(2)	2.255(8)	2.009(3)	2.261(8)	2.074(2)	2.045(3)	2.112(3)
M–X _A			2.221(2)		2.717(1)	2.027(2)	2.544(2)	2.028(3)	2.147(2)	2.147(2)	2.159(3)	2.069(2)
N3···N7	2.93	2.93	2.93	2.82	2.92	2.89	2.93	2.83	2.92	2.93	2.93	2.90
py1–M–py2	158.13(10)	155.62(16)	163.82(13)	148.81	160.07(7)	155.44	165.37(10)	148.53(11)	146.848(9)	153.2(9)	153.8(11)	153.35(8)
N3–M–X _E	165.02(7)	174.32(17)		175.82	160.82(7)	176.00	155.11(10)	154.39(13)		160.0(10)	174.8(11)	157.11(9)
N7–M–X _A			160.13(14)		169.89	170.09	155.01(10)	172.12(12)	157.64(6)	173.4(9)	165.0(11)	165.55(8)

^a This work.**Table 4.** Strain Energies (kJ/mol) of the Ligands L³ and L⁴, Induced by Their Coordination to Cu^{II} and Zn^{II}, Obtained by Single Point Calculations of the Relaxed X-ray or the Fully Optimized MM Structures, after Removal of the Metal Ions and Coligands (see Experimental Section)

	elongated N7–Cu–X _A		elongated N3–Cu–X _E		elongated py1–Cu–py2		Zn ^{II} complexes	
	X-ray	MM	X-ray	MM	X-ray	MM	X-ray	MM
L ³	92.75	84.09	96.84	102.03	92.69	109.83	84.69	
L ⁴	95.89	100.00	95.32	90.74	86.43	130.19	90.29	

For the copper(II) complexes of L⁴ and derivatives with various substituents at N7, there are also two isomers (“Jahn–Teller isomerism”) with an elongated N7–Cu–py3 or an elongated py1–Cu–py2 axis.¹⁵ For L⁴, the aqua complex has a short Cu–N7 bond (Cu–N3 = 2.056 Å, Cu–N7 = 2.072 Å, Cu–py1,2 = 2.3147/2.519 Å, Cu–py3 = 2.034 Å, Cu–OH₂ = 1.983 Å), and the chloro complex has a long Cu–N7 bond (Cu–N3 = 2.070 Å, Cu–N7 = 2.478 Å, Cu–py1,2 = 2.011/1.987 Å, Cu–py3 = 2.544 Å, Cu–Cl = 2.254 Å).^{8,15} The hexadentate ligand L⁵ forms copper(II) complexes with an elongated py1–Cu–py2 axis with a considerable asymmetry of the Jahn–Teller axis (Cu–N3 = 2.087 Å, Cu–N7 = 2.045 Å, Cu–py1 = 2.280 Å, Cu–py2 = 2.573 Å, Cu–py3 = 2.009 Å, Cu–py4 = 2.028 Å).²¹ Structural, spectroscopic, and computational studies indicate that the two isomeric copper(II) complexes of L⁴ are shallow minima on the potential energy surface and that the complex with an elongated py1–Cu–py2 axis is lower in energy.¹⁵

A reasonable qualitative interpretation of the copper(II) complex stabilities is that L³ has a high complementarity for copper(II), whereas the ligand–L⁴-based strain for copper(II) complexation with an elongated Cu–N7 and a weak Cu–py3 bond leads to considerable strain and therefore to a relatively low complex stability. The structure of the copper(II) complex with L⁵ is similar to that with L⁴, but the steric demand of the four pyridine donors leads to some steric crowding and concomitant distortions and strain.

The interesting question that then arises is why the order of complex stabilities with other metal ions without Jahn–Teller-labile electronic ground states also does not follow the naively expected pattern and is different from the copper(II) complexes; viz., the L⁴ complexes generally are more

stable than those with L³, which have similar stabilities to those with the hexadentate ligand L⁵ (see Co^{II}, Ni^{II}, and Zn^{II} in Table 2). We have checked the structural features specifically with the closed-shell zinc(II) (d¹⁰) systems and therefore have crystallized and structurally characterized structures with zinc(II), i.e., the isomers [Zn(L³)(OH₂)]²⁺ and [Zn(L⁴)(OH₂)]²⁺. The structural parameters of these and the known structures of L¹ (two isomers,² only one given in Table 3) and L⁵²¹ are presented, together with corresponding copper(II) structures in Table 3; plots of the two new structures are shown in Figure 2. An interesting observation is that the general trend of bond distances for copper(II) and zinc(II) complexes of L³ and L⁴ are similar. With L³ there are elongated bonds to N7 and X_A; with L⁴ the M–N3 and M–N7 bonds are similar in length and the M–py3 bond is relatively short, whereas the M–py1,2 bonds are relatively long. Note that with other metal ions similar trends are observed (e.g., high spin iron(II)) and that for other ligands, specifically for derivatives of L⁴ and their copper(II) complexes, there are different trends which are discussed elsewhere.¹ A possible interpretation is that the structures of the zinc(II) and copper(II) complexes of L³ (elongated N7–M–X_A axis) and L⁴ (elongated py1–M–py2 axis) are the result of ligand enforcement and that for copper(II), the metal-based electronic preferences are an additional perturbation to these structural effects.

This was further analyzed with a qualitative force field study. Here we concentrate on the zinc(II) and copper(II) complexes of ligands L³ and L⁴, which are isomers and therefore well-suited for a comparative molecular mechanics analysis (similar studies for L¹ and L²,² as well as for L⁵²¹ have been published). The isomers of the copper(II) and zinc(II) complexes were fully refined (the three possible “Jahn–Teller isomers” for the copper(II) complexes), and the ligand-based strain was calculated by single point calculations of the optimized structures with metal ions and coligands removed. The ligand-based strain was also computed from the crystal structural data after optimization of the structures with constrained positions of the metal ions and the six donor atoms. These data are assembled in Table 4. As expected from the stability constants and the structural data of the copper(II) complexes it appears that the geometry with an elongated M–N7 bond in complexes of L³ and a py1–M–py2 elongation with L⁴ is due to ligand preference. The

(21) Bleiholder, C.; Börzel, H.; Comba, P.; Ferrari, R.; Heydt, A.; Kerschler, M.; Kuwata, S.; Laurenczy, G.; Lawrance, G. A.; Lienke, A.; Martin, B.; Merz, M.; Nuber, B.; Pritzkow, H. *Inorg. Chem.* **2005**, *44*, 8145.

Table 5. Crystal Data and Structure Refinement for [Zn(L³)H₂O](ClO₄)₂ and [Zn(L⁴)H₂O](ClO₄)₂(H₂O)₂

	[Zn(L ³)H ₂ O](ClO ₄) ₂	[Zn(L ⁴)H ₂ O](ClO ₄) ₂ (H ₂ O) ₂
empirical formula	C ₂₈ H ₃₅ Cl ₂ N ₅ O ₁₆ Zn	C ₂₈ H ₃₉ Cl ₂ N ₅ O ₁₈ Zn
formula weight	833.88	869.91
temperature (K)	100(2)	100(2)
wavelength (Å)	0.71073	0.71073
crystal system	monoclinic	triclinic
space group	<i>P</i> 2 ₁ / <i>c</i>	<i>P</i> -1
<i>a</i> (Å)	19.3095(15)	11.0389(9)
<i>b</i> (Å)	11.5399(9)	13.3736(10)
<i>c</i> (Å)	16.0539(13)	13.4546(10)
α (deg)	90	82.410(1)
β (deg)	111.5130(10)	66.354(1)
γ (deg)	90	74.306(1)
volume (Å ³)	3328.1(5)	1751.1(2)
<i>Z</i>	4	2
density (calcd) (Mg·m ⁻³)	1.664	1.650
abs coeff (mm ⁻¹)	0.983	0.942
<i>F</i> ₀₀₀	1 720	900
crystal size (mm)	0.25 × 0.25 × 0.25	0.25 × 0.20 × 0.05
θ range for data collection (deg)	2.10–32.24	2.07–32.09
reflectns collected	65 334	41 976
indep reflectns	11 190 (<i>R</i> _{int} = 0.0487)	11 338 (<i>R</i> _{int} = 0.0280)
completeness to θ = 32.09° (%)	94.9	92.5
absorption correction	semiempirical from equivalents	semiempirical from equivalents
max and min transmission	0.7929 and 0.7912	0.9554 and 0.7886
refinement method	full-matrix least-squares on <i>F</i> ²	full-matrix least-squares on <i>F</i> ²
data/restraints/parameters	11 190/0/474	11 338/0/513
goodness-of-fit on <i>F</i> ²	1.086	1.104
final <i>R</i> indices (<i>I</i> > 2σ(<i>I</i>))	<i>R</i> 1 = 0.0436, w <i>R</i> 2 = 0.1128	<i>R</i> 1 = 0.0380, w <i>R</i> 2 = 0.1066
<i>R</i> indices (all data)	<i>R</i> 1 = 0.0625, w <i>R</i> 2 = 0.1229	<i>R</i> 1 = 0.0479, w <i>R</i> 2 = 0.1127
rms residual density	0.107	0.088
largest diff peak and hole (e ⁻ Å ⁻³)	1.329 and -1.171	1.602 and -1.159

differences in bond length are larger in the copper(II) than in the zinc(II) complexes (see Table 3), and this suggests that electronic effects are of importance in copper(II) but are not the only effect. The preferences of copper(II) for L³ and of zinc(II) for L⁴ are not primarily a result of steric effects. From an inspection of the structures (Figures 2 and 3), it appears that the third pyridine donor in the Cu^{II}L⁴ structure with an elongated N7–Cu–py3 axis is not well-oriented with respect to the Cu d_{z²} orbital and is expected to only form a very weak bond. This also emerges qualitatively from the spectroscopic and redox data. Therefore, it is not astonishing that the complex stability of this complex is similar to that of L¹.

The two isomers of [Cu(L⁴)(X)]²⁺ are compared in Figure 3. The isomer with an elongated N7–Cu–py3 axis (yellow structure) has Cl⁻ as the coligand, and repulsion between the coligand and the N7 substituent might be the reason for the destabilization of the electronically slightly preferred structure with a py1–Cu–py2 elongation. The copper(II) donor bonds are very different in the two structures (Cu–N7: 2.105/2.470 Å; Cu–py1,2: 2.353(2.260)/2.011(1.987)). Interestingly, the geometries of the bispidine backbone in the two isomers are nearly identical, and this is supported by similar ligand-based strain energies (see Table 4); the N3–N7 distances (2.89 vs 2.93 Å) and the valence angles around C2 and C4 (113.6, 113.9, 108.6, 109.3, 106.0, 105.5 vs 114.3, 115.6, 108.2, 110.4, 107.3, 107.4) are nearly unstrained. The main structural differences are found in the torsions around the C2,4–py1, py2 axes (-80.3, 74.9 vs -90.8, 96.2), which have low-energy barriers. The overlay plot in Figure 3 suggests that switching between the two isomers involves a small tilt (rotation of the bispidine

backbone around the C2–C4 axis) with a concomitant adjustment of the C2, C4–py1, py2 torsions. This clearly is a low-energy process; i.e., the two minima are shallow.

An interesting additional feature, not discussed here in detail but related to the ligand-enforced geometries, is that none of the ligands follows the Irving-Williams series of complex stabilities. That is, the cobalt(II) complexes generally are more stable than the corresponding nickel(II) compounds, and this might lead to interesting applications.

Conclusion

It is a general observation that structures of transition metal complexes and, consequently, the corresponding molecular properties (spectroscopic properties, reactivity, redox potentials, complex stabilities) are the result of a compromise between ligand and metal-ion-based preferences.^{22,23} Especially for rigid ligands, such as the bispidines, the ligand enforces the structure, and the only flexibility of the ligand is based on torsions around single bonds, most of which are blocked in the bicyclic bispidine systems. Therefore, the isomerism observed in the complexes of the ligands studied here only involves the positioning of the metal ion in the bispidine cavity—which is another way to describe the tilting of the bispidine backbone—with a concomitant adjustment of the pendant pyridine donors.

The unexpected and exciting trends of stability constants have been shown to be qualitatively related to structural effects and steric strain, and the stability constants are well-correlated with the redox potentials. Clearly, a quantitative

(22) Comba, P. *Coord. Chem. Rev.* **1999**, *182*, 343.

(23) Comba, P.; Schiek, W. *Coord. Chem. Rev.* **2003**, *238–239*, 21.

correlation also has to include electronic effects, which are an additional perturbation to the ligand-based steric effects. These and their relative importance are currently analyzed on the basis of a combined ligand field and DFT analysis, coupled to force field calculations.

Experimental Section

Syntheses. All ligands and the corresponding metal complexes were prepared according to published procedures.^{8,9,21}

Copper(I) Stability Constants. To different amounts of $[\text{Cu}(\text{CH}_3\text{-CN})_4]\text{BF}_4$, weighted in NMR tubes, were given 400 μL of a 25 mM solution of the ligand in deuterated acetonitrile under argon atmosphere. Upon complexation, the color of the samples changed from colorless to yellow, which is typical for the Cu^{I} -bispidine complexes. Constant ionic strength was maintained with 0.1 M KCl. The samples were mixed, and $^1\text{H-NMR}$ spectra were measured with a 250 MHz Bruker ARX 200 NMR spectrometer at room temperature. Sixty-four scans were recorded with a spectral width of 15 ppm. At least five different ratios of ligand to copper were analyzed per ligand.

Copper(II) Stability Constants. Potentiometric titrations were performed on 20 cm^3 samples with metal ion concentrations of 1.0×10^{-3} and 5.0×10^{-3} mol dm^{-3} and a metal to ligand ratio of 1:1. The measurements were made with a pH meter equipped with a 6.0202.100 combined electrode (Metrohm) and a 665 Dosimat automatic burette (Metrohm), containing a carbonate-free stock solution of tetrabutylammonium hydroxide of ~ 0.1 M, standardized by titration of potassium hydrogen phthalate. For each measurement 120–200 titration points were recorded. During the titration, a slight nitrogen stream was passed over the sample solution to ensure the absence of carbon dioxide. All pH measurements were carried out at a constant ionic strength ($\mu = 0.1 \text{ mol dm}^{-3}$ KCl) and constant temperature ($T = 298$ K, $\text{p}K_{\text{w}} = -13.78$). The overall stability constants were calculated with Hyperquad and Specfit, which also included absorbance data, recorded simultaneously by a TIDAS II (J&M) spectrophotometer, equipped with an external immersion probe 661.202UVS from Hellma. The proton equilibrium was also analyzed by Bjerrum charts.²⁴ For each system, each titration was repeated at least twice with good reproducibility ($\sim \pm 0.01$ pH units). At low pH retro-Mannich reactions might be a problem, but this was not observed. However, at higher pH values L^3 decomposes to a product with an intense yellow color. The differences between equivalence points in the titration of the metal-free ligands are those expected for the weighed quantities (see Supporting Information). For the determination of the formation constants with Cu^{2+} , there was a small amount of Cu^+ not complexed from the very beginning of the experiments, which made it difficult to optimize the stability constants based on pH values alone. Therefore, we attempted to determine the constants through 1:1:1 ligand–ligand–metal competition titrations. Various competing ligands with known $\text{p}K_{\text{a}}$ values and complex formation constants (EDTA (1,2-diaminoethane- N,N,N',N' -tetraethanoic acid),^{25–27} NTPH (nitrilotris(methylphosphonic acid)),^{28,29} and PMIDA ((N -phosphonomethyl)iminodiethanoic acid)³⁰) were used in these experiments. However, titration

based on the competition between various bispidine ligands was more efficient (L^3 vs L^4 for the formation of CuL^4 and L^1 vs L^2 for the formation of CuL^1).

Cyclic Voltammetry. Electrochemical measurements were obtained from a BAS100B system with a glassy-carbon working, a Pt-wire auxiliary, and an (i) Ag/AgCl or (ii) Ag/AgNO₃ reference electrode. All complexes were measured in degassed acetonitrile (for (i)) or water (for (ii)) with 0.1 M tetrabutylammonium hexafluorophosphate (for (i)), or 0.1 M KNO₃ (for (ii)) with a scan rate of 100 mV/s. The potential of the Fc^+/Fc couple is at 86 mV for (i) and 172 mV for (ii).

Crystal Structure Determination. A 0.2 g (0.39 mM) portion of L^3 or L^4 was solved in 3 mL methanol, and 0.15 g (0.41 mM) of $\text{Zn}(\text{ClO}_4)_2(\text{H}_2\text{O})_6$ in methanol (2 mL) was added under stirring. After 1 h at 4 °C colorless crystals were obtained and analyzed by elemental analyses and subsequent X-ray structure determination was made. Single crystals of $\text{ZnL}^3(\text{H}_2\text{O})(\text{ClO}_4)_2 \cdot \text{H}_2\text{O}$ and $\text{ZnL}^4(\text{H}_2\text{O})(\text{ClO}_4)_2 \cdot 3\text{H}_2\text{O}$ were prepared directly from the reaction mixtures. The crystals of $\text{ZnL}^4(\text{H}_2\text{O})(\text{ClO}_4)_2 \cdot 3\text{H}_2\text{O}$ so obtained were monoclinic and of space group $C2/c$. On standing in the presence of solvent for several days, a triclinic polymorph of $\text{ZnL}^4(\text{H}_2\text{O})(\text{ClO}_4)_2 \cdot 3\text{H}_2\text{O}$ (space group $P1$) crystallized. Crystal data are given in Table 5. Intensity data were collected for $\text{ZnL}^3(\text{H}_2\text{O})(\text{ClO}_4)_2 \cdot \text{H}_2\text{O}$ and both forms of $\text{ZnL}^4(\text{H}_2\text{O})(\text{ClO}_4)_2 \cdot 3\text{H}_2\text{O}$ on a Bruker AXS SMART 1000 CCD diffractometer at low temperature. The data were corrected for absorption and other effects.³¹ The structures were solved by combined heavy atom and direct methods³² and refined by full matrix least-squares analysis based on F^2 .³³ All non-hydrogen atoms were given anisotropic displacement parameters. Hydrogen atoms were input in calculated positions. The hydrogen positions of the coordinated water molecules were taken from Fourier maps but were not refined. Hydrogen atoms of the solvent water molecules could be neither found nor unambiguously calculated.

The data set obtained from the monoclinic form of $\text{ZnL}^4(\text{H}_2\text{O})(\text{ClO}_4)_2 \cdot 3\text{H}_2\text{O}$ was of rather low quality, as judged from its low mean intensity and high R_{int} . The structure was solved but could not be satisfactorily refined. The gross structure is similar to the triclinic form (including the solvent water molecules), the main difference being that there is a different orientation of one of the C(O)OME groups.

Crystallographic data (excluding structure factors) for the structure reported in this paper have been deposited with the Cambridge Crystallographic Data Center as supplementary publications CCDC 630987 and 630988. Copies of the data can be obtained free of charge on application to The Director, CCDC, 12 Union Road, Cambridge CB2 1EZ, UK (Telefax Int.+1223/336-033; e-mail: teched@chemcrs.cam.ac.uk).

Force Field Calculations: Force field calculations were done with the MOMECS program³⁴ and force field³⁵ specific parameters for copper(II) bispidine complexes were as used before.^{2,4,21} Note that copper–bispidine parameters are not fully refined. For the

(24) Avdjeev, A. *Curr. Top. Med. Chem.* **2001**, *1*, 277.

(25) Delgado, R.; Quintino, S.; Teixeira, M. *J. Chem. Soc., Dalton Trans.* **1997**, 55.

(26) Anderegg, G. *IUPAC Chem. Data Ser.* **1978**, 14.

(27) Baumann, E. *J. Inorg. Nucl. Chem.* **1974**, *36*, 1827.

(28) Sawada, K.; Miyagawa, K.; Sakaguchi, T. *J. Chem. Soc., Dalton Trans.* **1993**, 3777.

(29) Sawada, K.; Araki, T.; Suzuki, T. *Inorg. Chem.* **1989**, *28*, 2687.

(30) Dhansay, M.; Linder, P. *J. Coord. Chem.* **1993**, *28*, 133.

(31) Sheldrick, G. M. *SADABS-2004/1*, Bruker AXS; University of Göttingen: Göttingen, Germany, 2004.

(32) Beurskens, P. T.; Beurskens, G.; de Gelder, R.; Ganda, S. G.; Gould, R. O.; Israel, R.; Smits, J. M. M. *DIRDIF-99*; University of Nijmegen: Nijmegen, The Netherlands, 1999.

(33) Sheldrick, G. M. *SHELXS-97 Program for Structure Solution; SHELXL-97 Program for Structure Refinement*; University of Göttingen: Göttingen, Germany, 1997.

(34) Comba, P.; Hambley, T. W.; Okon, N.; Lauer, G. *MOMECS97, a Molecular Modeling Package for Inorganic Compounds*; VCH Publishers: Heidelberg, Germany, 1997.

(35) Bol, J. E.; Buning, C.; Comba, P.; Reedijk, J.; Ströhle, M. *J. Comput. Chem.* **1998**, *19*, 512.

starting structures, crystal structural data of copper(II)–bispidine complexes with MeCN as coligand were used along with the ester groups at C₁ and C₅ (see Scheme 1) as well as the hydroxide groups at C₉ substituted by hydrogen atoms. The strain of the ligands in these complexes was calculated after optimization of the backbone with constraints on the metal ion and the six donor atoms, and the single point calculations were performed after removal of the metal ion and coligands (=X-ray in Table 4). The entries MM in Table 4 are from fully refined structures, where the Jahn–Teller axis has been assigned by the atom types available in MOMECC. Calculations on the zinc complexes were performed in the same way, starting

from the corresponding X-ray crystal structures but without definition of the elongated axis.

Acknowledgment. Financial support by the German Science Foundation (DFG) is gratefully acknowledged.

Supporting Information Available: ¹H-NMR spectroscopic data and titration curves, as well as protonation and stability constants for all species. This material is available free of charge via the Internet at <http://pubs.acs.org>.

IC061501+